High-Definition X-Ray Polarimetry

Berit Marx

IOQ
Friedrich-Schiller-Universität Jena

Helmholtz-Institut Jena

Workshop - EMMI

I.Uschmann, S. Höfer, R. Loetzsch, O. Wehrhan, E. Förster, M. Kaluza, G.G. Paulus, C. Detlefs, T. Roth, J. Härtwig

Outline

Vacuum birefringence induced by intense laser fields

Experimental setup for the verification of vacuum birefringence:

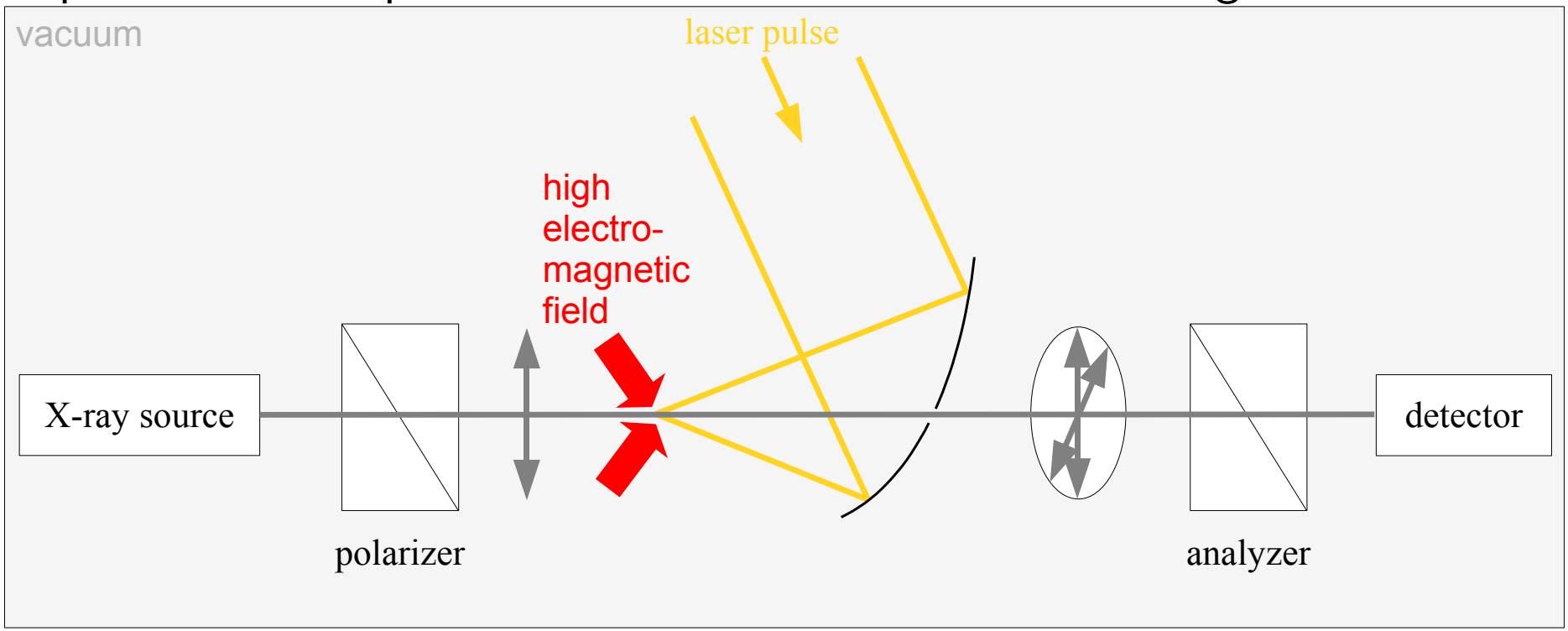

T. Heinzel et al. 2006

Vacuum birefringence induced by intense laser fields

resulting ellipticity δ

$$\delta^2 \cong \frac{2\alpha}{15}\frac{z_0}{\lambda}\frac{I_0}{I_C}\kappa$$

T. Heinzel et al. 2006

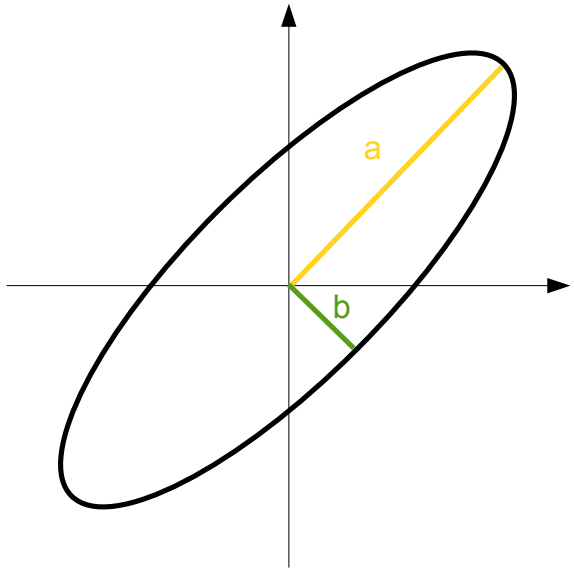

I_0-peak intensity
λ-probe pulse wavelength
z_0-Rayleigh length
α-fine-structure constant
κ-correction factor
I_C-critical intensity

Ellipticity, which would be possible with the petawatt laser system at Jena:

$I_0 = 10^{22}\frac{W}{cm^2}$
$\lambda = 0.08nm$
$z_0 = 25\mu m$
$\Rightarrow \delta^2 = 4.8 \cdot 10^{-10}$

Outline

Kinematical theory

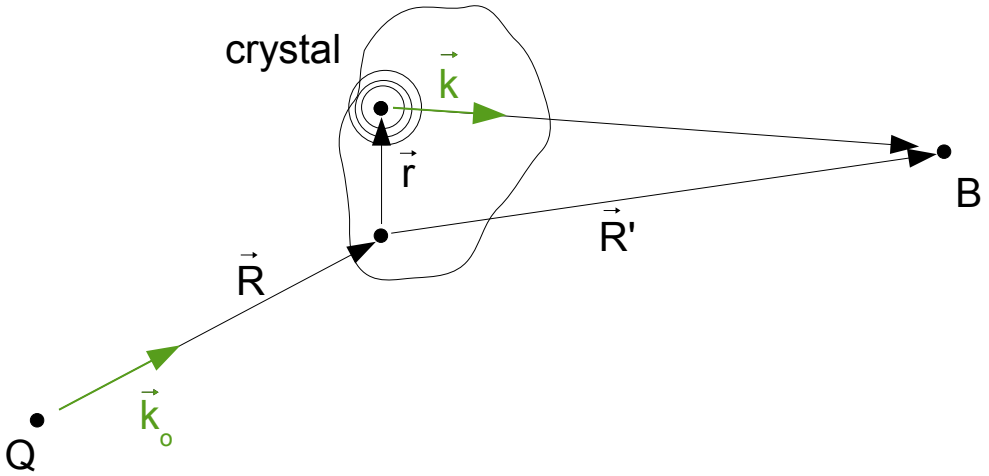

fig.: Diffraction

- no change of wavenumber in the crystal
- decrease of intensity of the primary beam is neglected
- no secondary scattering
  $\Rightarrow$ only valid for mosaic crystals and thin crystals

Intensity of the diffracted beam at the observation place

$$I(\vec{K}) \cong \frac{|A_0|^2}{\vec{R'}^2} \left| \sum_{\vec{G}} \rho_{\vec{G}} \int e^{i(\vec{G}-\vec{K})\vec{r}} d\vec{r} \right|^2 \quad with \quad \vec{K} = \vec{k} - \vec{k}_0$$

Diffraction condition

Laue condition

$$\vec{G} = \vec{k} - \vec{k}_0$$

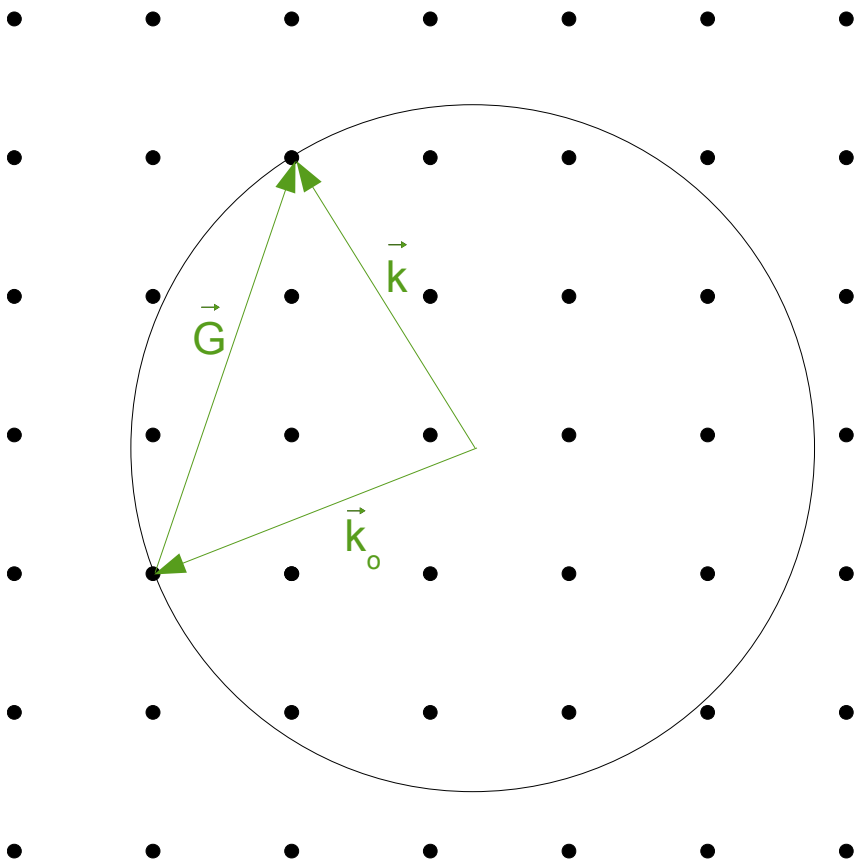

Diffraction condition

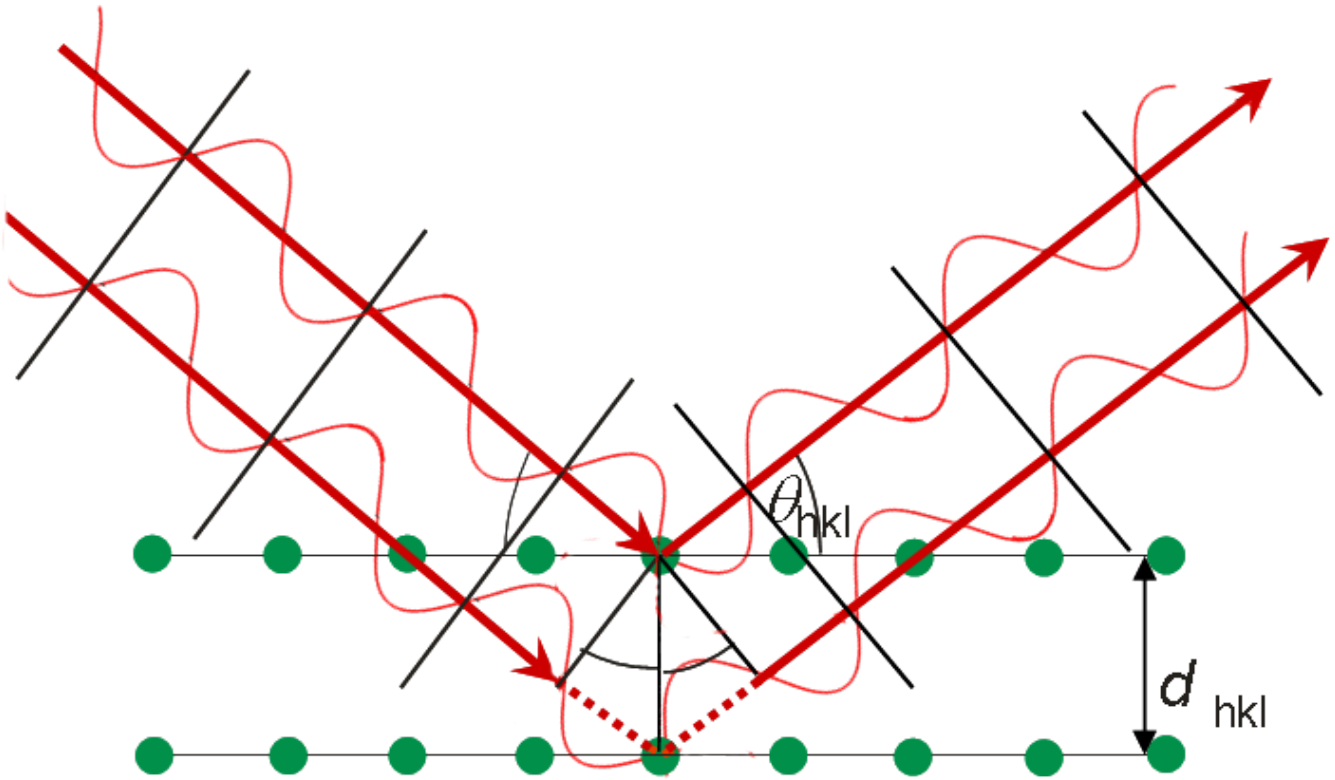

Bragg's law

$$2d_{hkl}sin(\theta_{B_{hkl}}) = n\lambda$$

Outline

Dynamical theory of diffraction

- solves Maxwell's equations for the propagation of electromagnetic waves in the crystal
  $\Rightarrow$is valid for perfect crystals

Dynamical theory of diffraction

- solves Maxwell's equations for the propagation of electromagnetic waves in the crystal
  ⇒is valid for perfect crystals

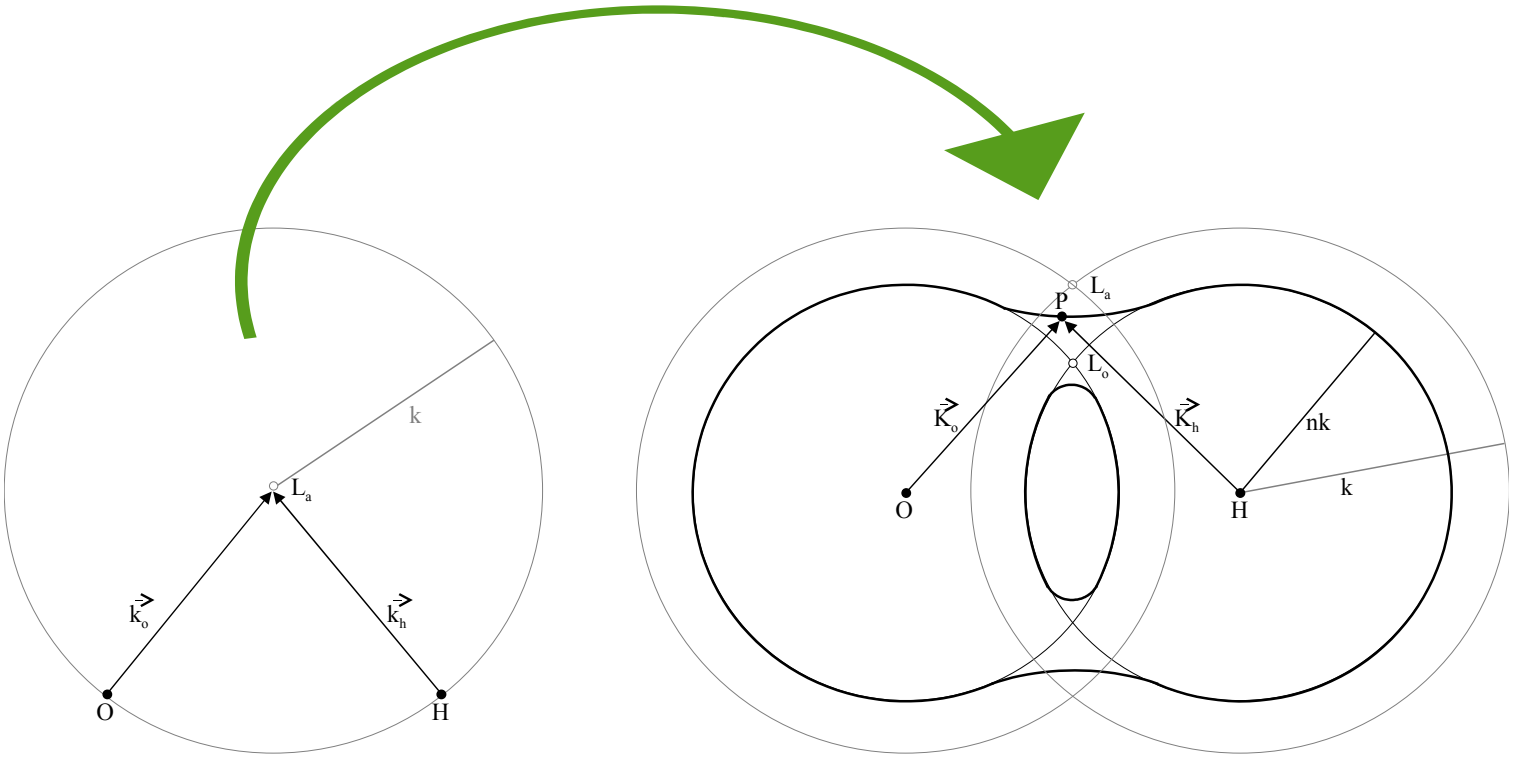

fig.: —Dispersion surface

Integrated intensity of a perfect crystal

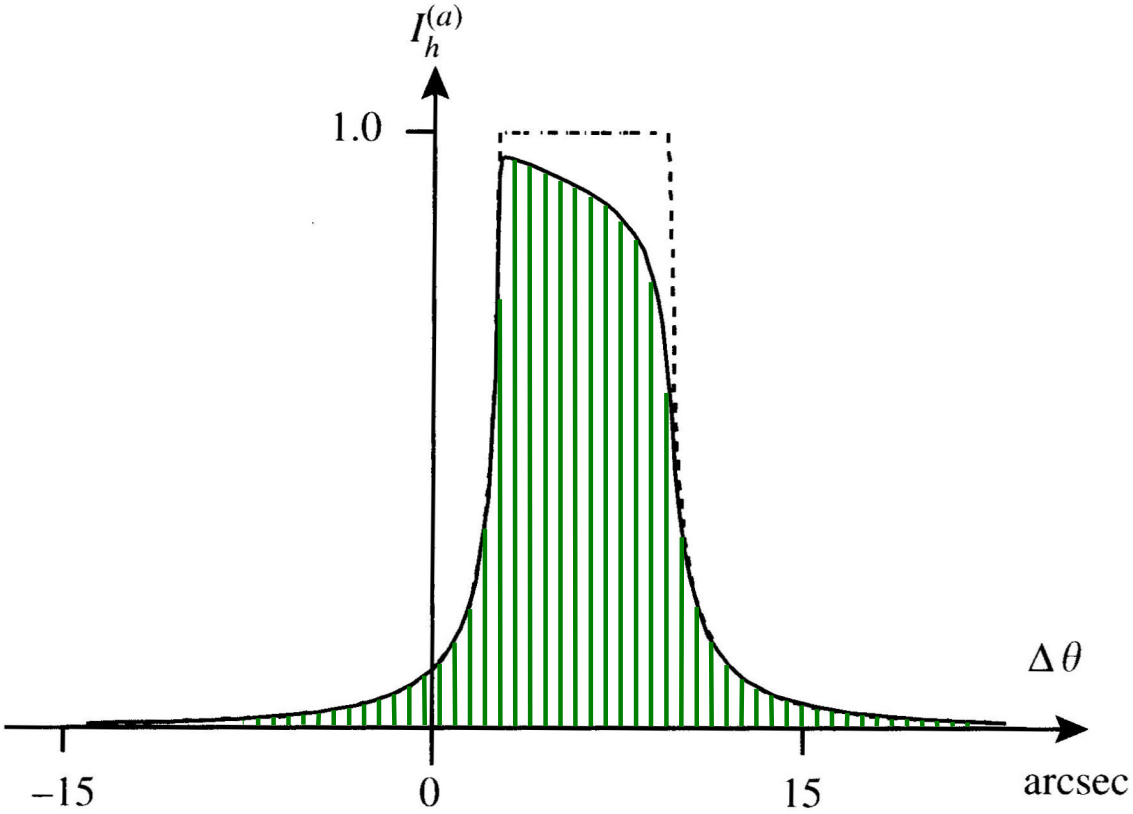

fig.: Comparison of the rocking curves for
· · ·non-absorbing
—-absorbing crystals

Integrated intensity

$$R_{\sigma/\pi} = \frac{8R\lambda^2 |C| \sqrt{|\gamma|}}{\pi V sin(2\theta_B)} \sqrt{F_h F_{\bar{h}}}$$

Integrated intensity of a perfect crystal

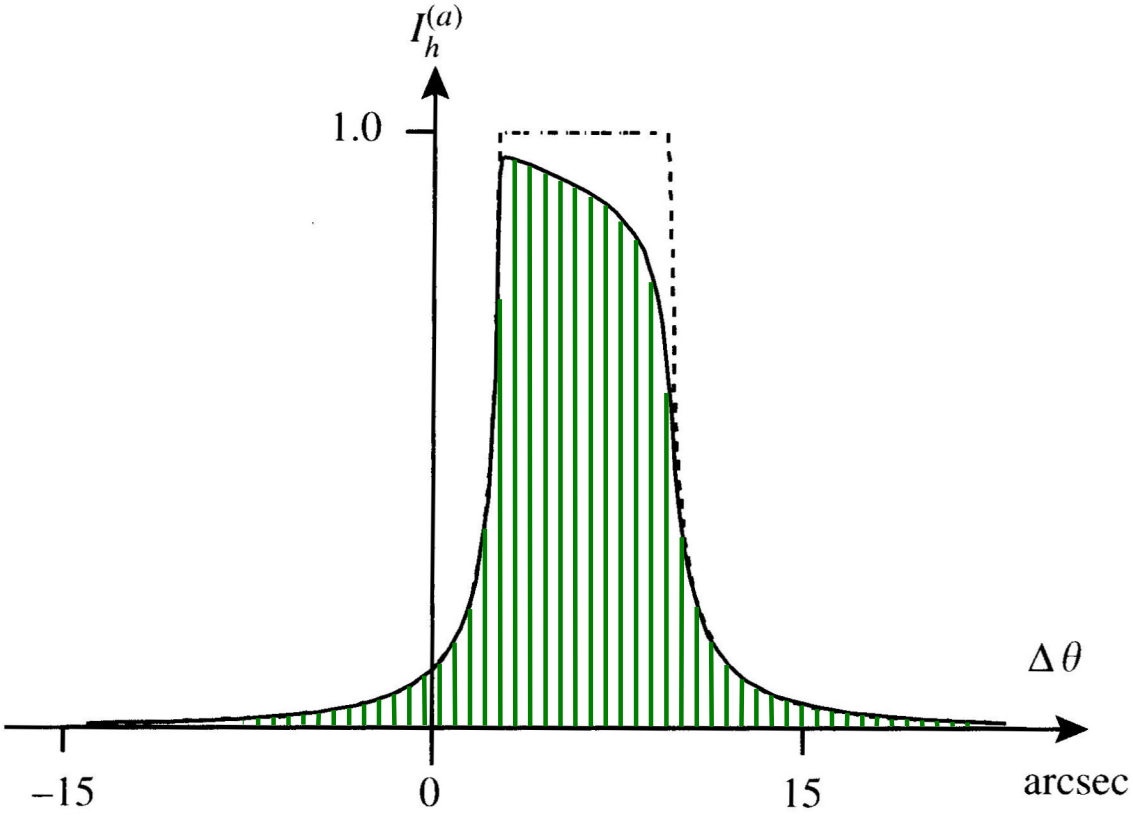

fig.: Comparison of the rocking curves for
· · ·non-absorbing
—-absorbing crystals

Integrated intensity

$$R_{\sigma/\pi} = \frac{8R\lambda^2 |C| \sqrt{|\gamma|}}{\pi V sin(2\theta_B)} \sqrt{F_h F_{\bar{h}}}$$

Polarization factor

$$C = \begin{cases} 1 & \text{for } \sigma \\ cos2\theta_B & \text{for } \pi \end{cases}$$

$\Rightarrow$ Suppression of the π-polarization at $\theta_B = 45°$

Integrated intensity of a perfect crystal

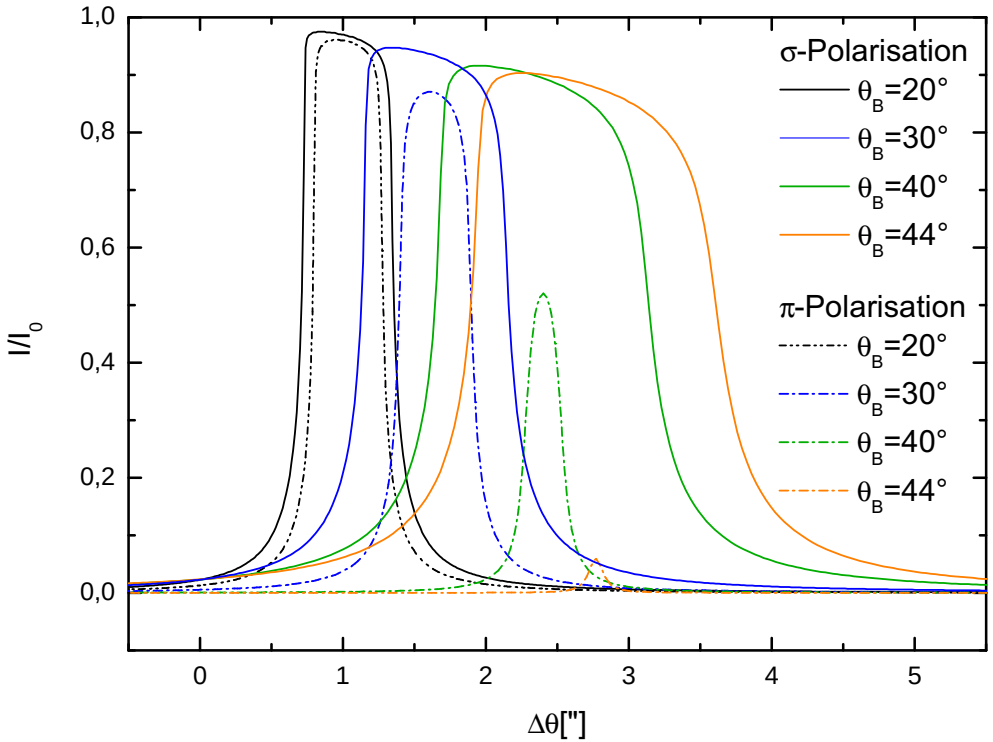

fig.: Comparison of rocking curves for different Bragg angles

Integrated intensity

$$R_{\sigma/\pi} = \frac{8R\lambda^2 |C| \sqrt{|\gamma|}}{\pi V sin(2\theta_B)} \sqrt{F_h F_{\bar{h}}}$$

Polarization factor

$$C = \begin{cases} 1 & \text{for } \sigma \\ cos2\theta_B & \text{for } \pi \end{cases}$$

$\Rightarrow$ Suppression of the π-polarization at $\theta_B = 45°$

Outline

Polarization purity

Transmitted flux

$$T_{(\pi,\sigma)} = \int\int I^{n}_{(\pi,\sigma)}(\theta, E_0+\epsilon)B(\theta, E_0+\epsilon)d\theta d\epsilon$$

$B(\theta, E_0 + \epsilon)$	-	spectral brilliance
E_0	-	Bragg energy
θ	-	angle arround θ_B(Bragg angle)
$I_{(\pi,\sigma)}(\theta, E_0 + \epsilon)$	-	single-crystal reflectivity
n	-	number of reflections inside the channel-cut

Polarization purity

$$\delta_0 = \frac{T_\pi}{T_\sigma}$$

Suppression of π -polarization

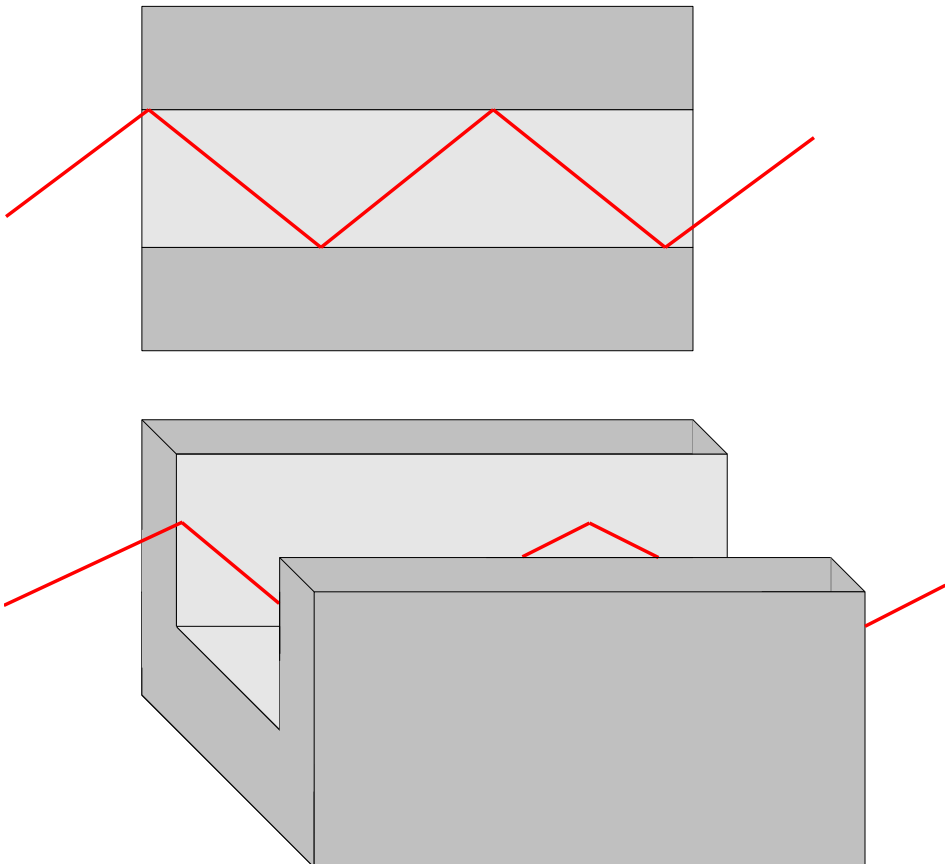

Si 333, Cu Kα, $\theta_B = 47.5°$

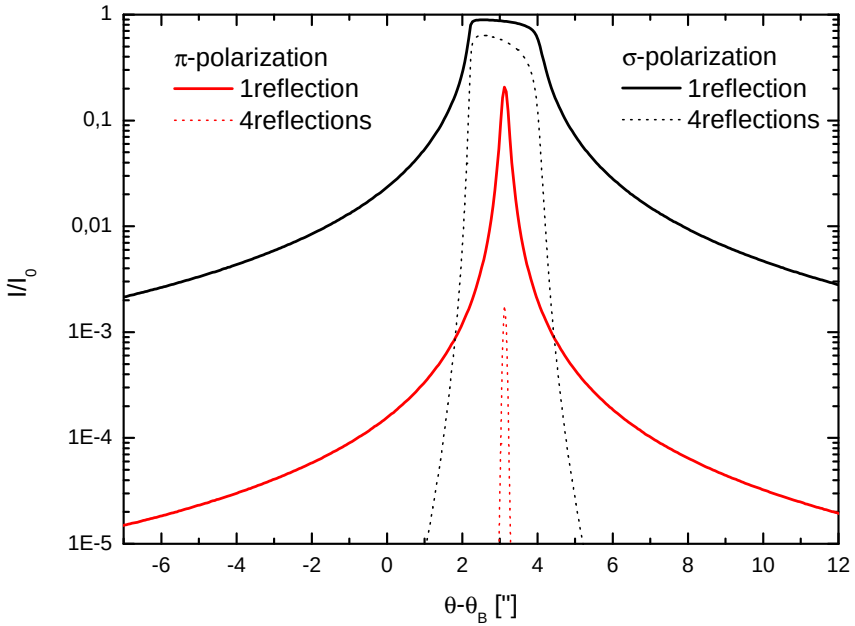

fig.: multiple reflections

$\delta_1 = 2,91 \cdot 10^{-2} \leftrightarrow \delta_4 = 2,20 \cdot 10^{-4}$

Multiple scattering

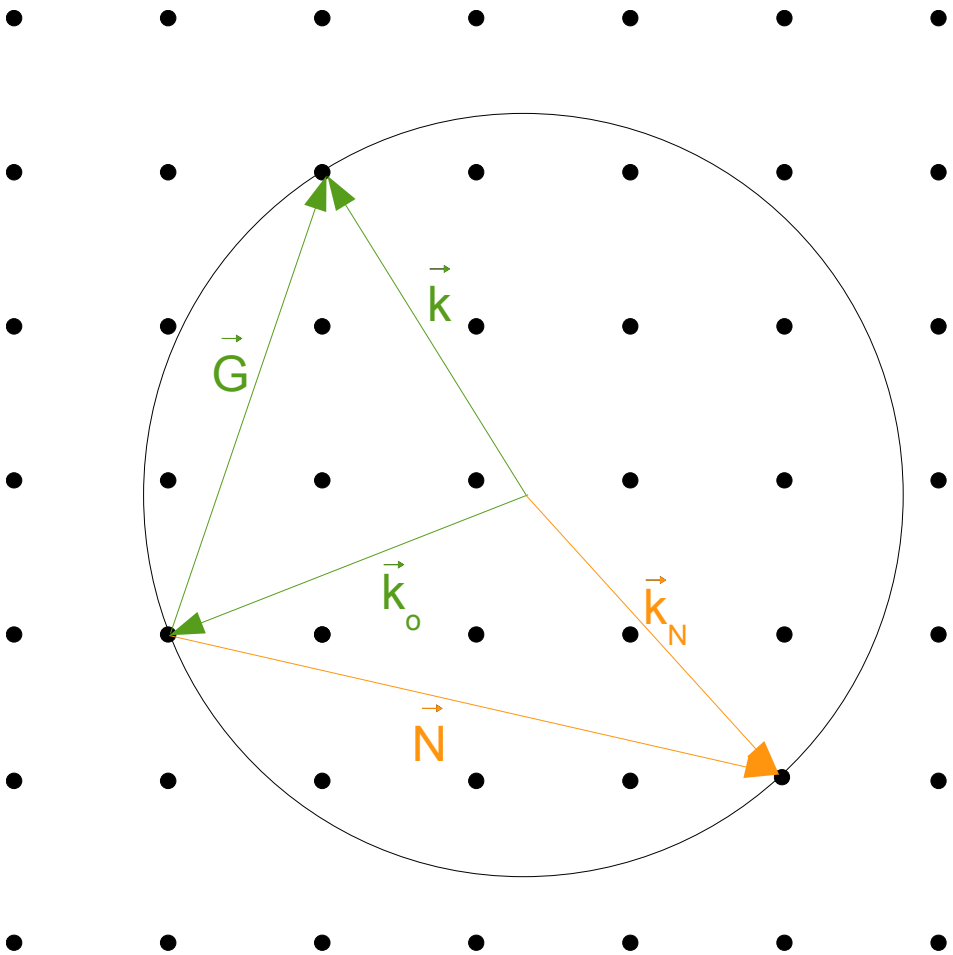

fig.: Appearance of multiple scattering demonstrated at the Ewald sphere

Umweganregungen

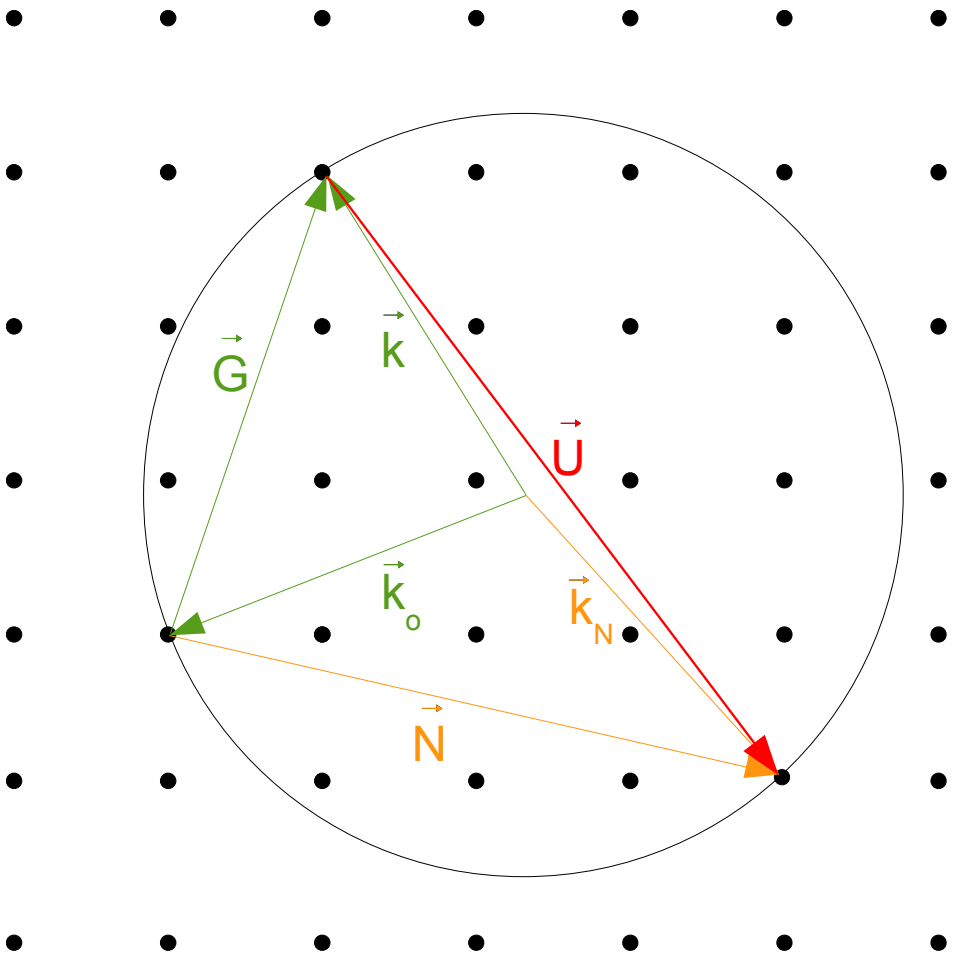

fig.: Appearance of indirect reflections demonstrated at the Ewald sphere

Multiple scattering

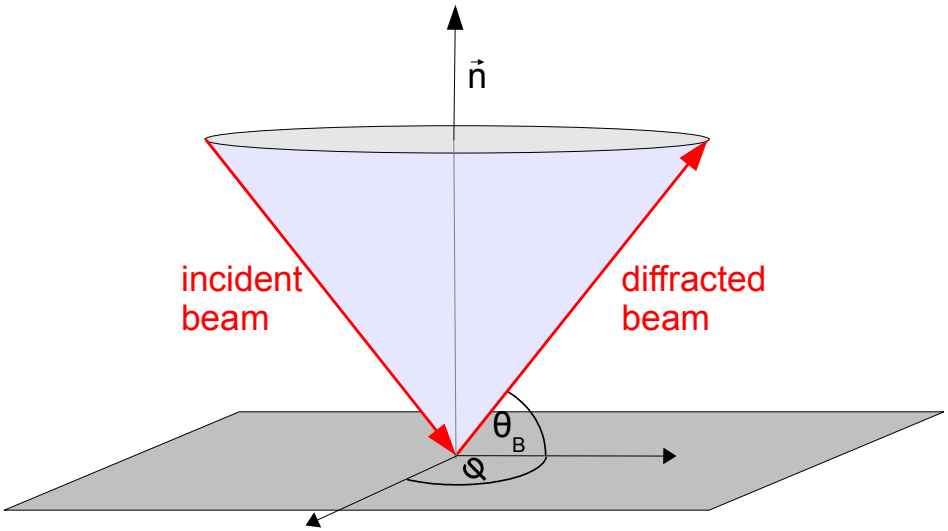

fig.: Kossel cone

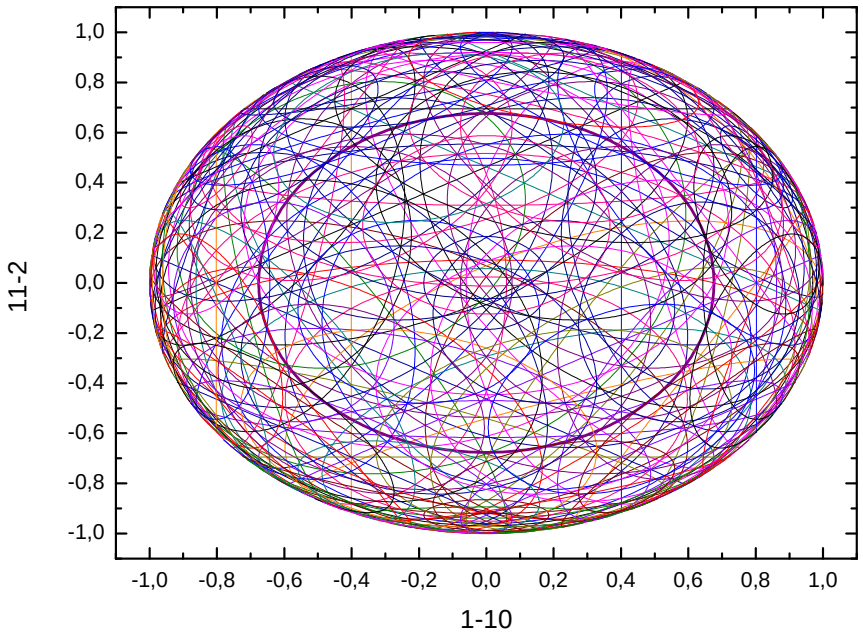

fig.: Kossel pattern of a (333) silicon crystal, CuKα, E=8.05keV

Multiple scattering

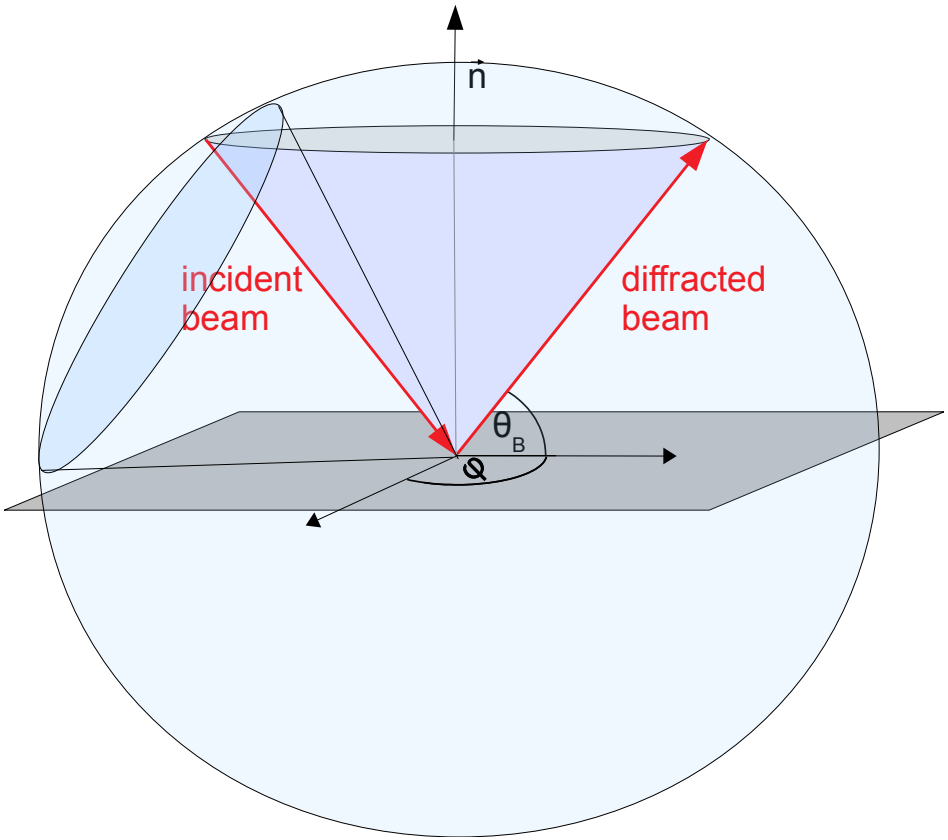

fig.: Kossel cone

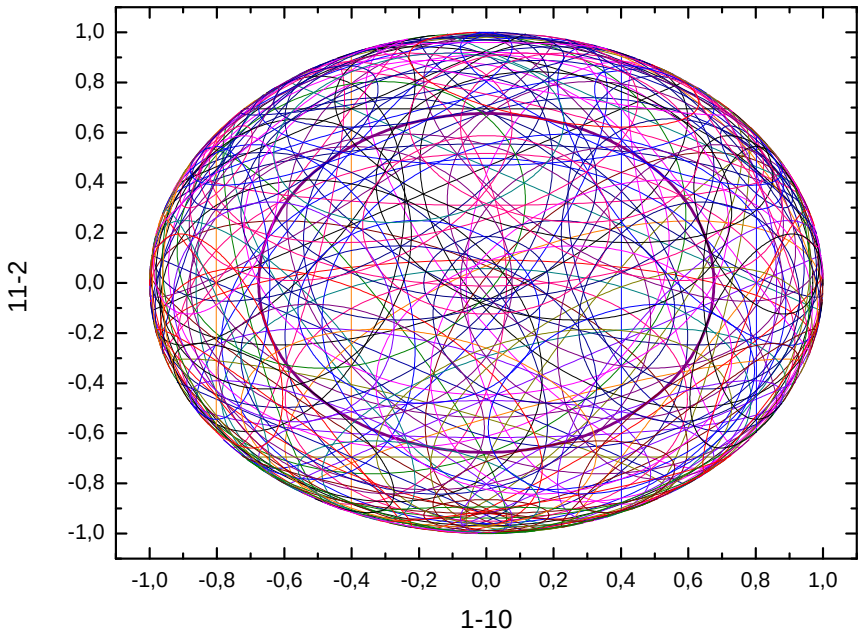

fig.: Kossel pattern of a (333) silicon crystal, CuKα, E=8.05keV

Umweganregungen

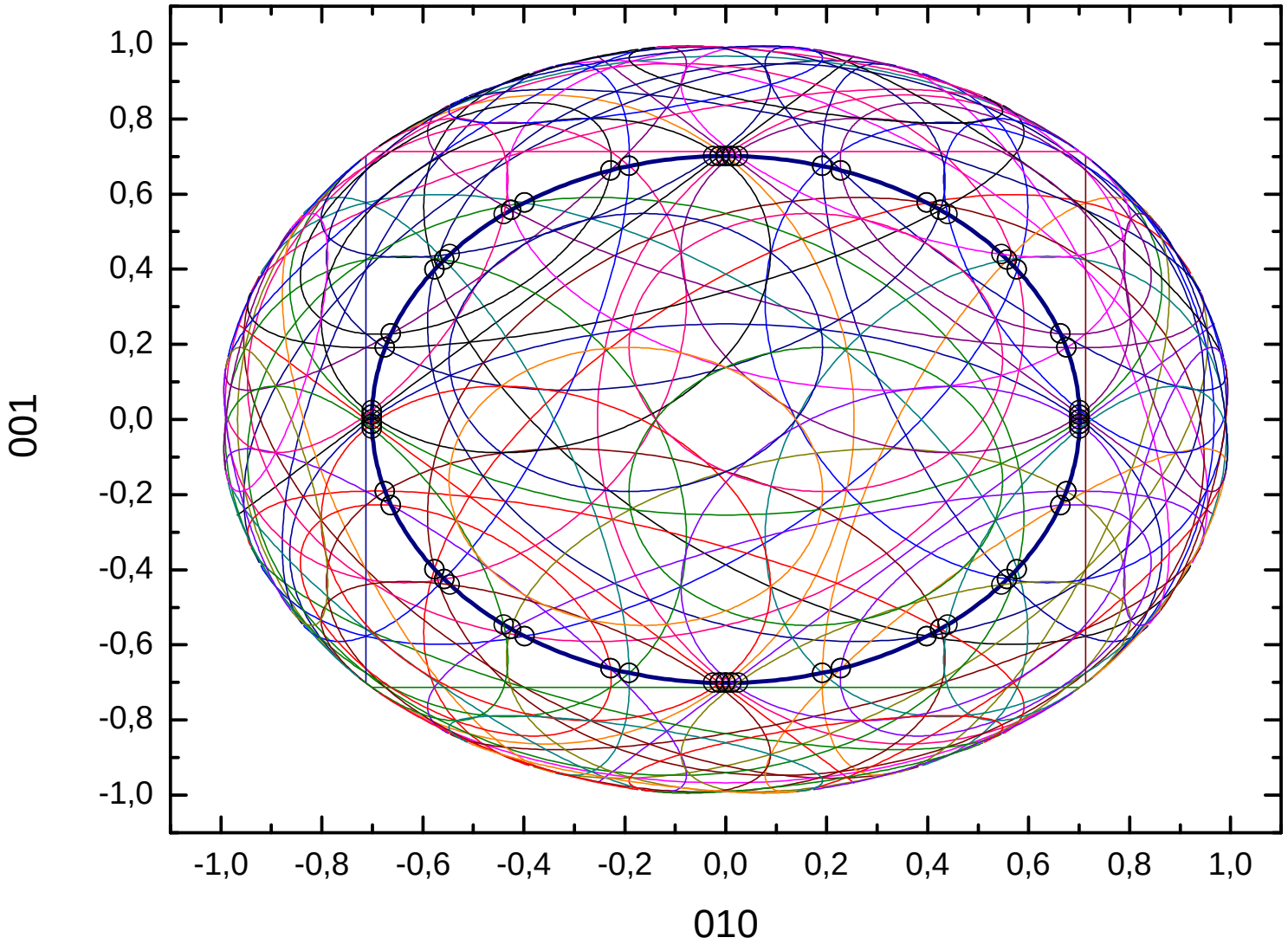

fig.: Kossel pattern of a (400) silicon crystal, FeKα, E=6.4keV, $\theta_B = 45,48°$

Umweganregungen

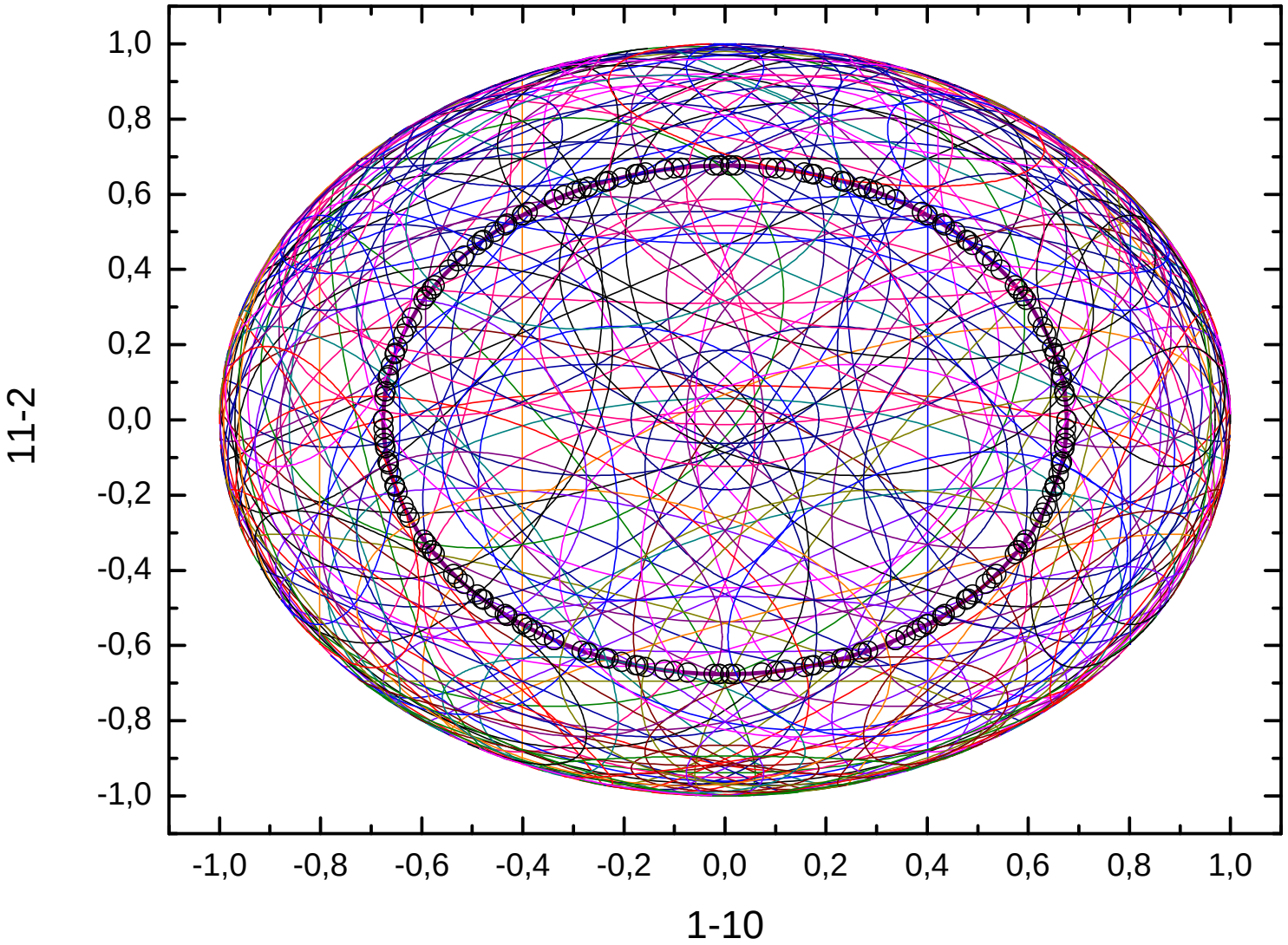

fig.: Kossel pattern of a (333) silicon crystal, CuKα, E=8.05keV, $\theta_B = 47,5°$

Umweganregungen

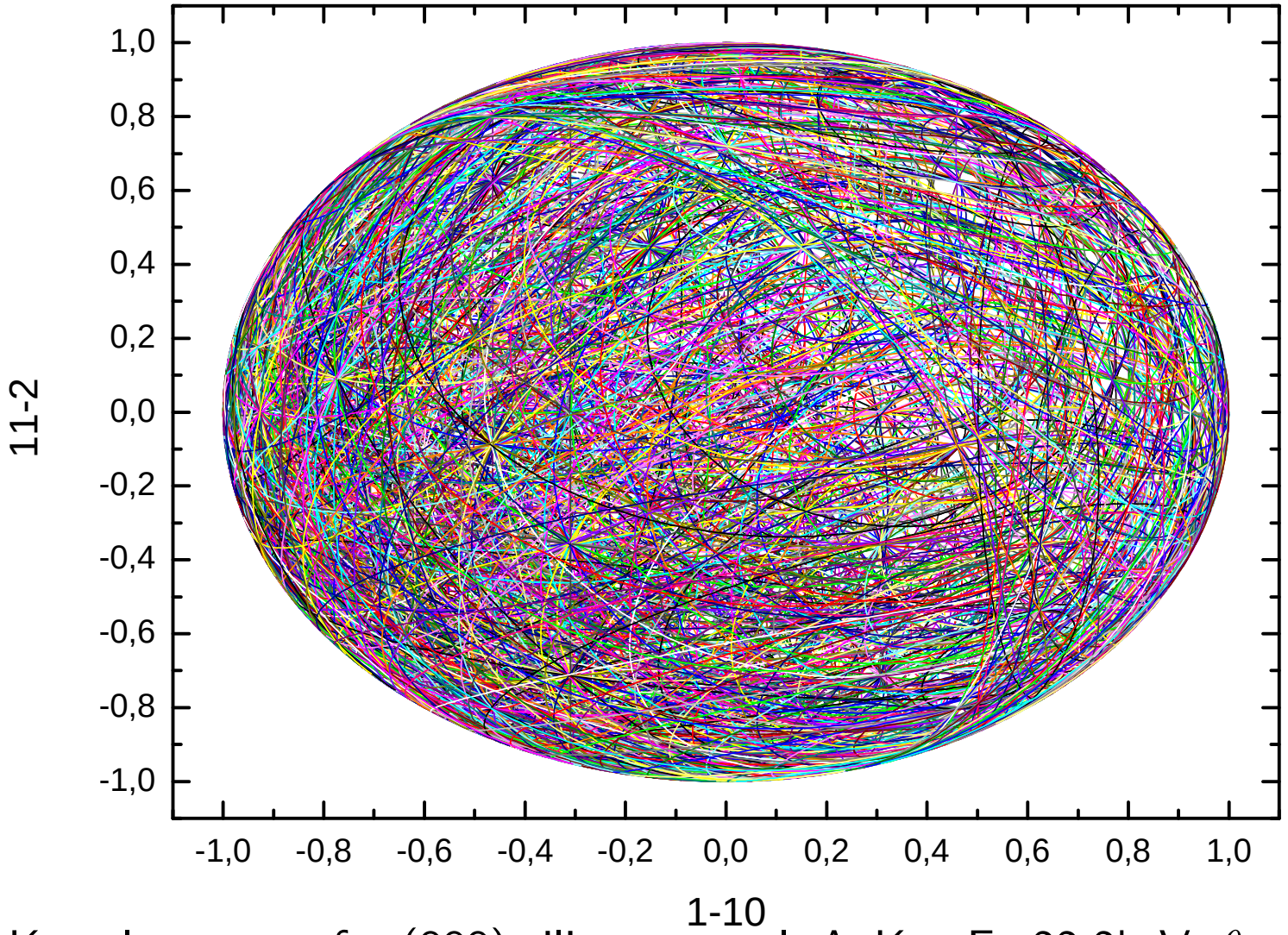

fig.: Kossel pattern of a (888) silicon crystal, AgKα, E=22.2keV, $\theta_B = 45,53°$

Polarimeter setup: polarizer

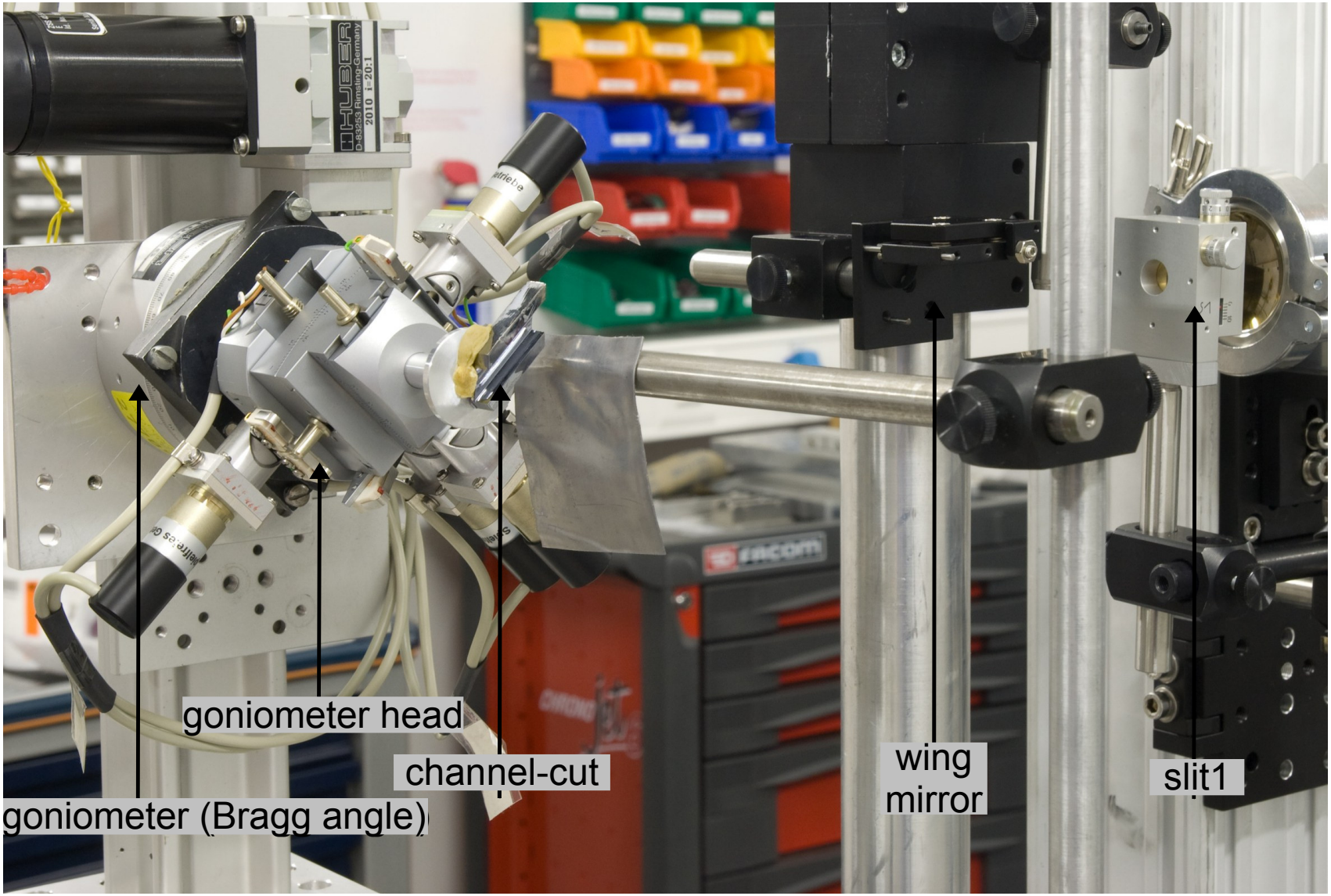

Polarimeter setup: analyzer

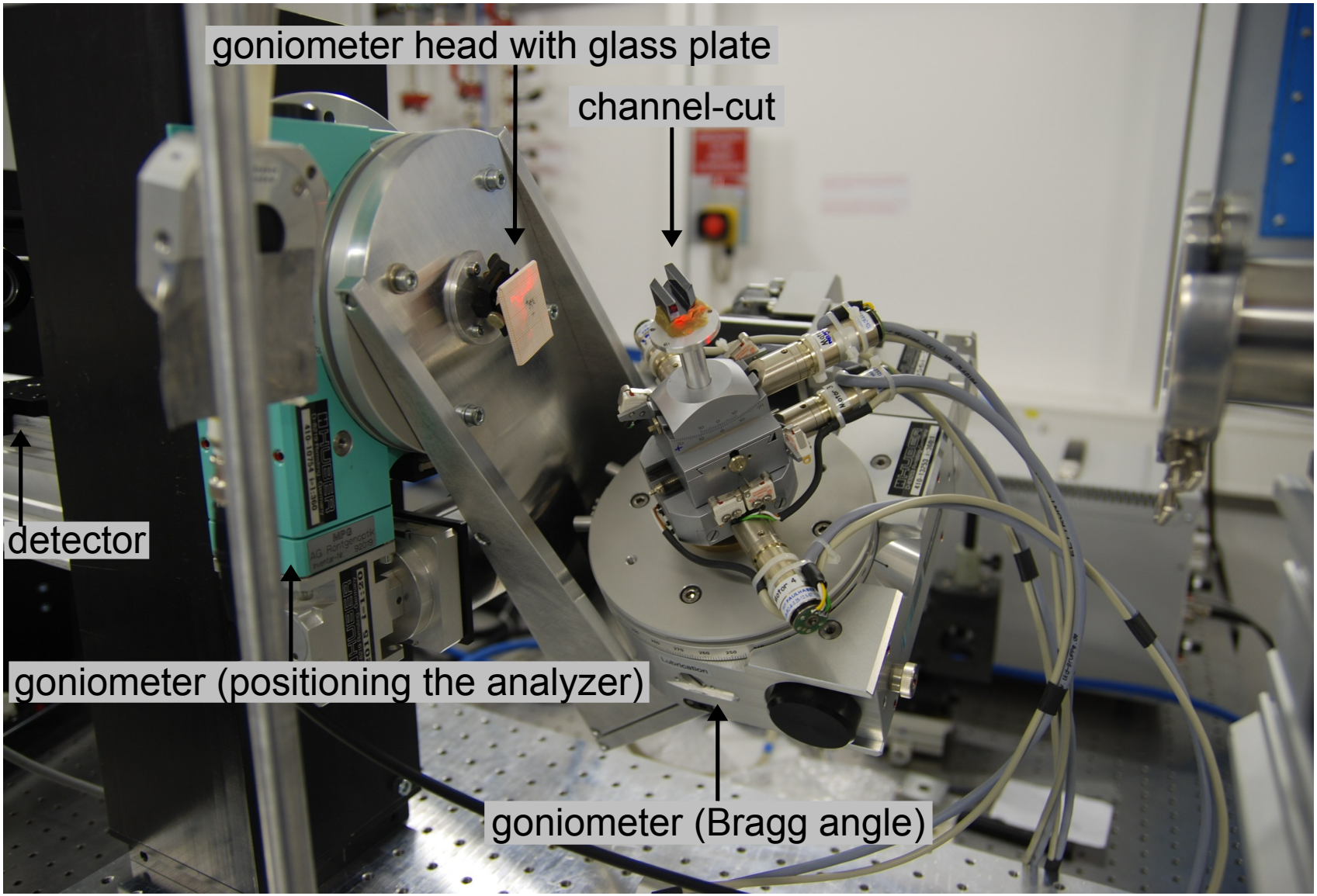

Outline

ESRF

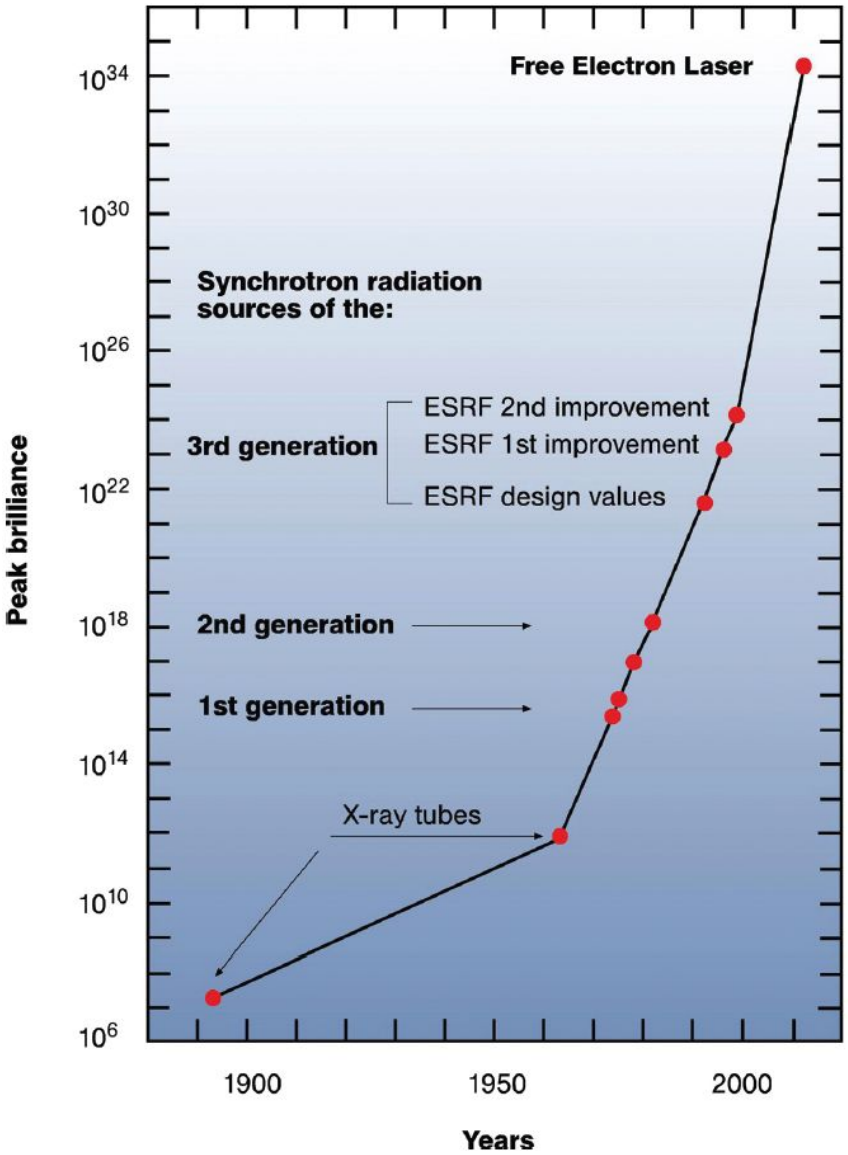

http://www.xfel.eu/

http://www.saxier.org/

Source parameters

- 16 bunch filling mode, $I < 90mA$
- beam is premonochromized (Si 111 2 reflections)
- vertical divergence $4.35\mu rad$
- horizontal divergence $15.45\mu rad$
- 2 undulators ($< 10keV, > 10keV$)
- Number of photons: $10^{10}\frac{ph}{s} - 10^{12}\frac{ph}{s}$

Setting up the wavelength

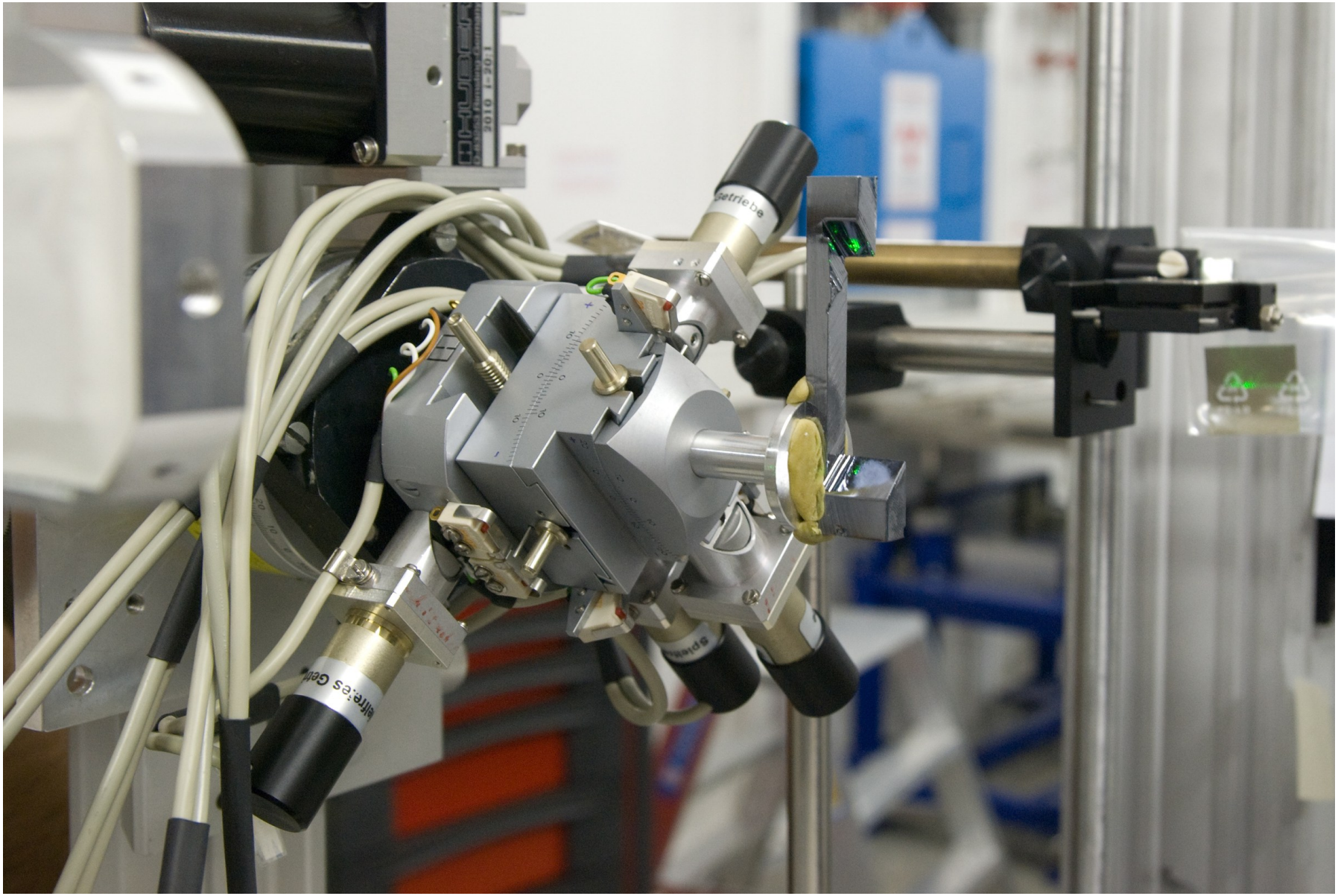

Principle of measurement

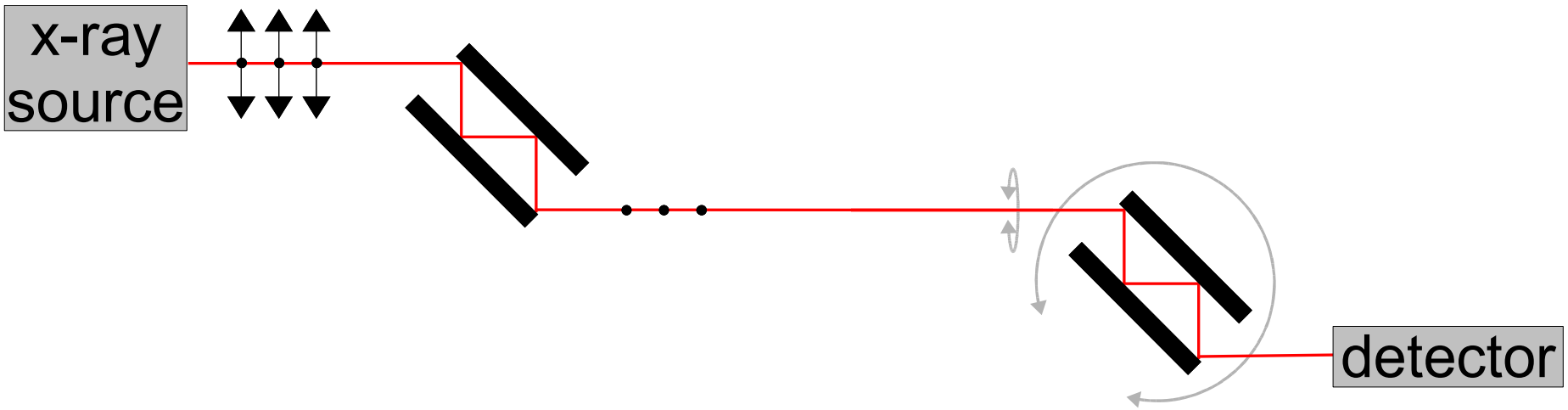

Principle of measurement

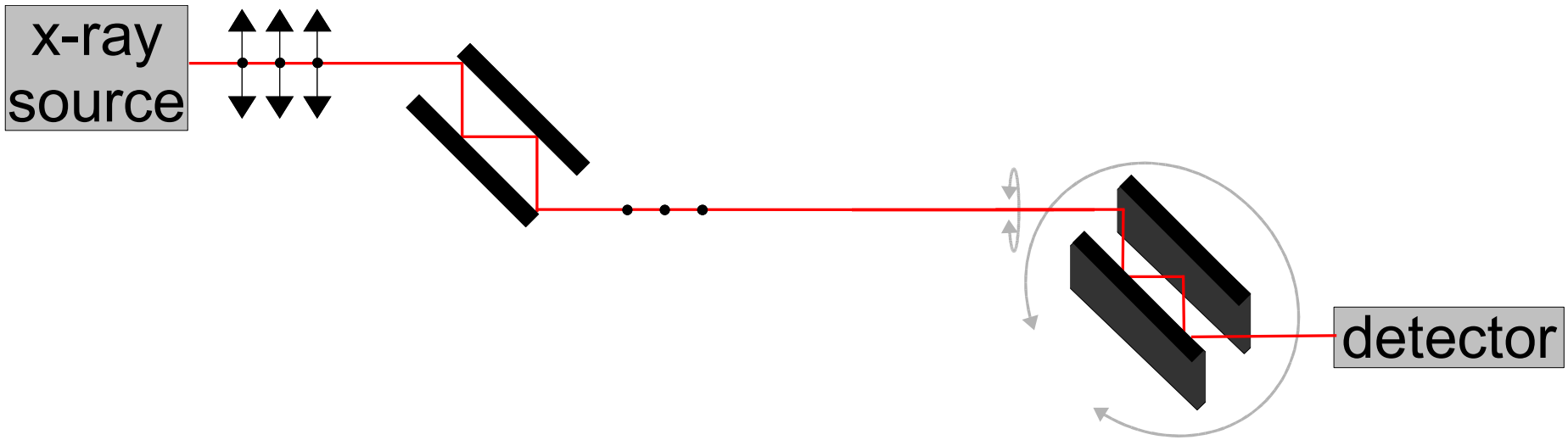

Principle of measurement

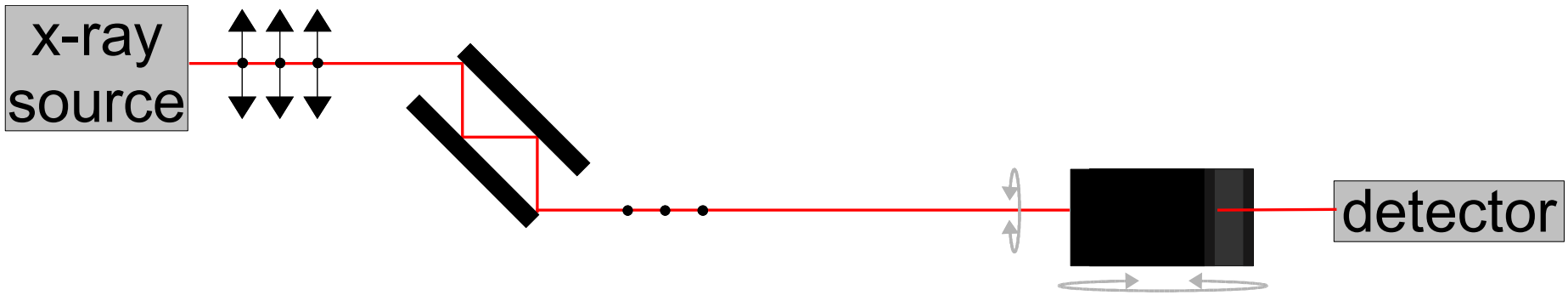

Results polarization purity

Intensity suppression for Si(400) with E=6.457keV ($\theta_B = 45.000°$).

Results polarization purity

Intensity suppression for Si(800) with E=12.914keV ($\theta_B = 45.000°$).

Varying the polarizer azimuth

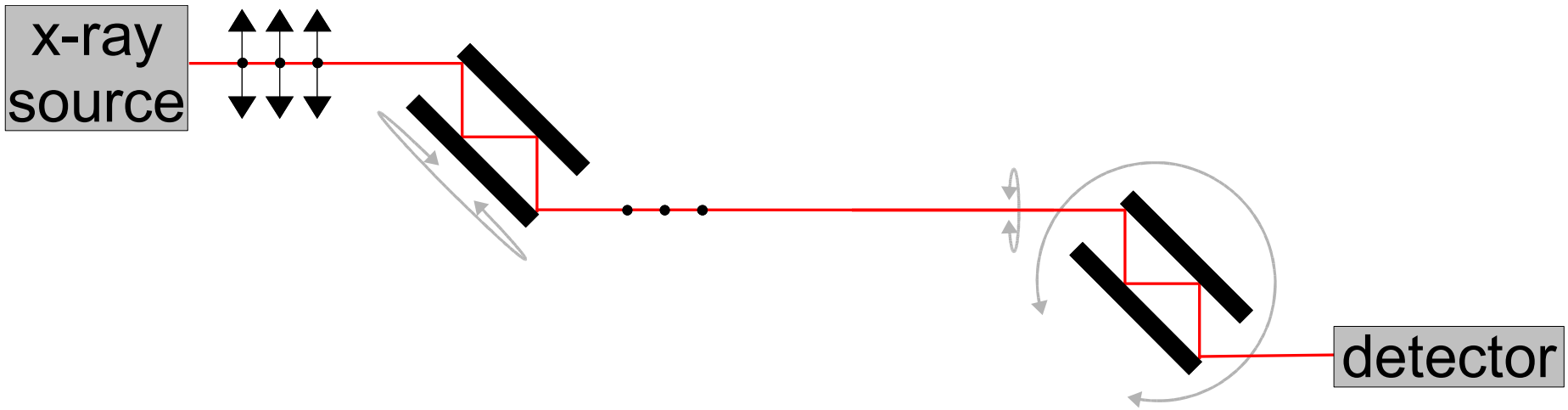

Varying the polarizer azimuth

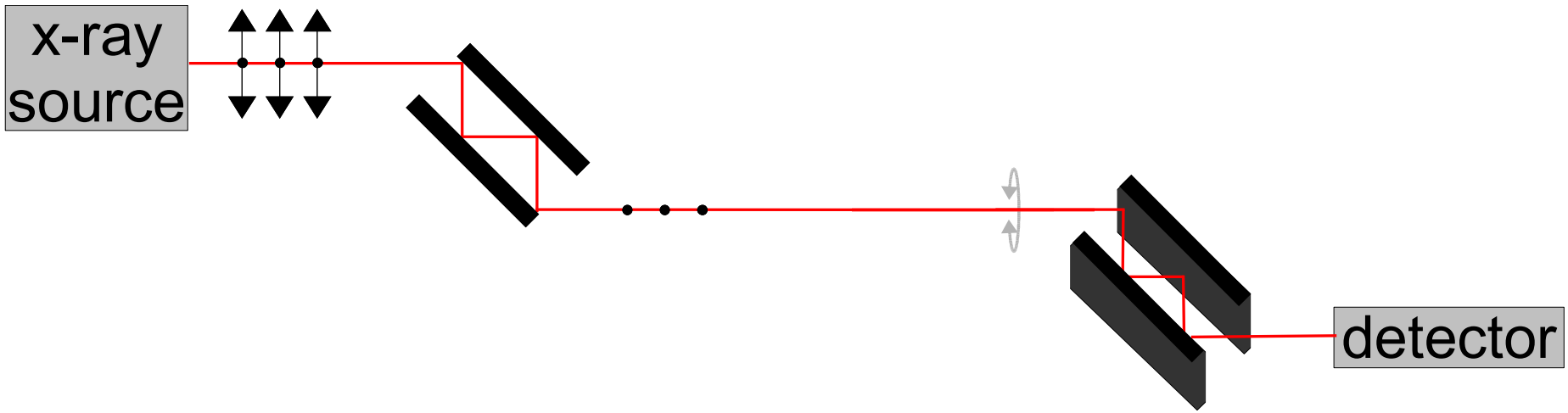

Varying the polarizer azimuth

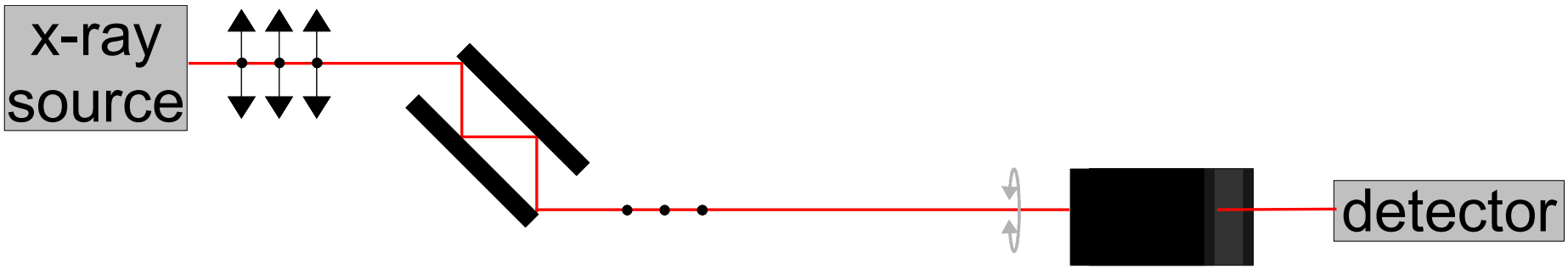

Rocking curves dependending on the analyzer position

Intensity suppression for Si(444) by varying the polarizer azimuth at E=11.1838keV.

Summary

Outlook

- polarization measurement at the ESRF using
  - more reflections (6,8)
  - other materials
  - crystal cooling
- full theoretical description of the polarimeter

Acknowledgement

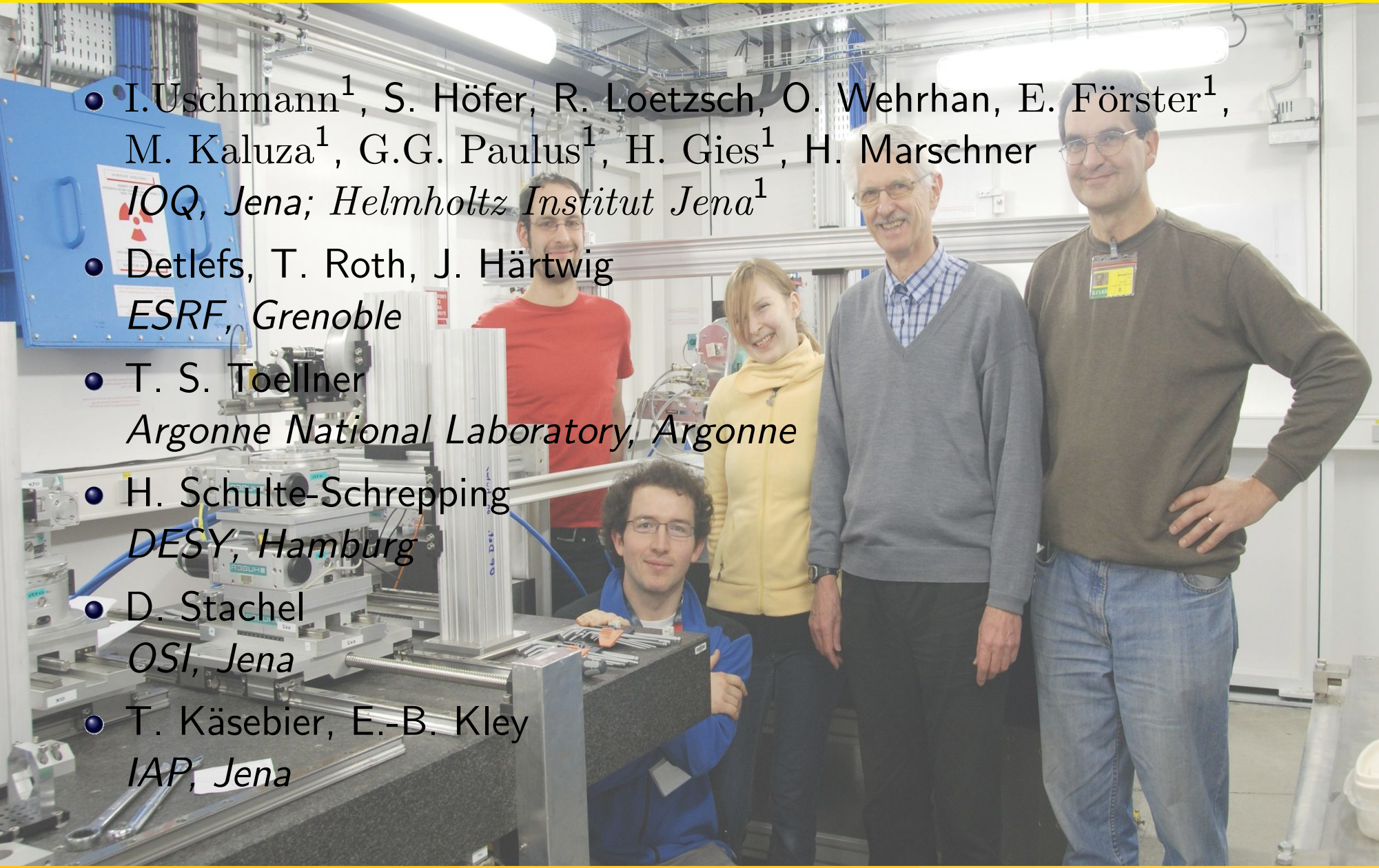

- I.Uschmann[1], S. Höfer, R. Loetzsch, O. Wehrhan, E. Förster[1], M. Kaluza[1], G.G. Paulus[1], H. Gies[1], H. Marschner
  IOQ, Jena; Helmholtz Institut Jena[1]
- Detlefs, T. Roth, J. Härtwig
  ESRF, Grenoble
- T. S. Toellner
  Argonne National Laboratory, Argonne
- H. Schulte-Schrepping
  DESY, Hamburg
- D. Stachel
  OSI, Jena
- T. Käsebier, E.-B. Kley
  IAP, Jena